Discriminating sources and preservation of organic matter in surface sediments from five Antarctic lakes in the Fildes Peninsula (King George Island) by lipid biomarkers and compound-specific isotopic analysis

Daniel Carrizo [a,*], Laura Sánchez-García [a], Rodrigo Javier Menes [b], Felipe García-Rodríguez [c,d]

[a] Centro de Astrobiología (CSIC-INTA), Madrid, Spain
[b] Laboratorio de Ecología Microbiana Medioambiental, Microbiología, Facultad de Química y Facultad de Ciencias, Universidad de la República, Uruguay
[c] Centro Universitário Regional Este, CURE-Rocha, Universidad de la República, Ruta 9 y Ruta 15 s/n, Uruguay
[d] Programa de Pós-Graduação em Oceanografia Física, Química e Geológica, Instituto de Oceanografia, Universidade Federal do Rio Grande, Av. Itália, km 8, Cx.P. 474, 96201-900 Rio Grande, RS, Brazil

HIGHLIGHTS

- Geochemical study on surface sediments from five Antarctic lakes, Fildes Peninsula
- Terrestrial lipid biomarkers were detected in all lakes.
- Aquatic-source indicators were relatively abundant in mid-size lakes near the glacier.
- Biogenic carbon was dominant in deep lakes whereas petrogenic carbon in shallow lakes.
- Distance to Collins Glacier, proximity to coast & lake depth are determinant factors in biogeochemical signature.

GRAPHICAL ABSTRACT
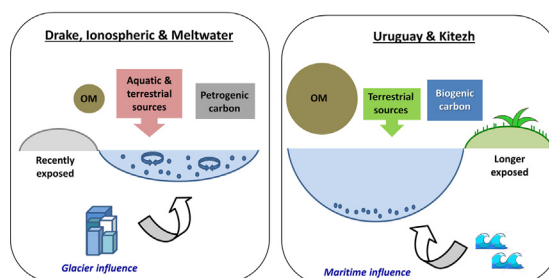
ARTICLE INFO

ABSTRACT

Lakes are important paleoenvironmental archives retaining abundant information due to their typical high sedimentation rates and susceptibility to environmental changes. Here, we scrutinize the organic matter (OM) composition, origin and preservation state in surface sediments from five lakes in a remote, warming-sensitive, and poorly explored region partially covered by the retreating Collins Glacier in King George Island (Antarctica), the Fildes Peninsula. Lipid biomarkers of terrestrial origin (i.e. high-molecular weight n-alkanes, n-alkanoic acids, and n-alkanols; β-sitosterol, campesterol, and stigmasterol) were detected in the five Fildes Lakes, with the smallest basin (i.e., Meltwater) showing a particularly strong moss imprint. Aquatic source indicators such as low C/N and terrestrial over aquatic ratios (TAR), or less negative $\delta^{13}C$ values were preferentially found in the mid-sized lakes (i.e., Drake and Ionospheric). Sedimentary carbon in the larger lakes (i.e., Uruguay and Kitezh) displayed a largely biogenic origin (i.e., values of carbon preference index, CPI, ≫1), whereas the three lakes close to Collins Glacier (i.e., Drake, Meltwater, and Ionospheric) showed certain contribution from petrogenic sources (CPI ~ 1). The results suggest that the geochemical signature of the surface sediments in the five Fildes lakes is determined by factors such as the distance to the retreating Collins Glacier, the proximity to the coast, or the lake depth. This study illustrates the forensic interest of combining lipid biomarkers, compound-specific isotopic analysis, and bulk geochemistry to reconstruct paleoenvironments and study climate-sensitive regions.

* Corresponding author.
E-mail address: dcarrizo@cab.inta-csic.es (D. Carrizo).

1. Introduction

Lakes are important paleoenvironmental archives of short-term processes at local to regional scale. They are systems susceptible to environmental changes (e.g. climate change, land uses, glacier retreatment, volcanic activity, biota, or human impact) that affect OM delivery and burial, thus imprinting the sedimentary record. Lakes receive abundant land-derived material that enhances lake fertility and aquatic production of OM, both producing high sedimentation rates that allow for retaining information from the water basement and catchment area. Lacustrine sediments constitute an integrative record of all local biogeochemical and geophysical processes (Cohen, 2003) with a variety of indicators or proxies that can be used to reconstruct past climate and environmental conditions.

A substantial arsenal of biomarker compounds, together with patterns of compound classes and the isotopic compositions of bulk OM or specific molecules enable to deduce much about the past ecosystems and environments in which the sedimentary OM was created and deposited (e.g., Freeman et al., 1994; Huang et al., 1996; Lamb et al., 2006; Arbi et al., 2018). Lipid biomarkers have been widely used to reconstruct paleoenvironments and changes in lacustrine systems (e.g. Arts et al., 2009; Vogts et al., 2009; Castañeda and Schouten, 2011; Ouyang et al., 2015), where different indexes have been developed as indicators of source and alteration of sedimentary OM (Cranwell, 1973; Simoneit et al., 1991; Meyers, 2003; Pancost and Boot, 2004). The OM signature is a mixture of compounds from different sources with a variable degree of preservation, susceptible to change upon diagenesis and biological alteration during sinking. Therefore, biomarkers interpretation has to be always done with caution, where the combination of multiple geochemical proxies helps to overcome these effects and thereby optimize paleoenvironmental and paleoecological reconstructions.

Antarctica is one of the most susceptible areas to climate and environmental changes due to the vast extensions of permanent ice, yet the most remote and unexplored continent on Earth. In particular, Maritime Antarctica is severely affected by climate change with ice melting and glaciers retreating in an accelerated way upon the current global warming. Over the last 40–50 years, the western and northern parts of the Antarctica Peninsula has experienced some of the most rapid air temperature increases (~2 °C; Quayle et al., 2002 Thomas and Tetzner, 2018), causing the thawing of large ice volumes and the retreatment of many glaciers. As a consequence, the system is becoming more humid, especially in the maritime Antarctica, where small streams and lakes fed by glacial and snow meltwater arise increasingly during austral summer. Most of these lakes have limited outflow and are supplied by surficial stream inflow as well as groundwater (Malandrino et al., 2009), carrying debris and particulate material from the surroundings. Subaqueous sediments in Antarctic glacial lakes may be considered as integrators of the short-term effects (decades to centuries) of the recent thermal destabilization.

Because of the great vulnerability of Antarctica, special protection figures were created by the Antarctic Treaty System in 1964 (i.e. Antarctic Specially Protected Areas or ASPA). One of these ASPA sites (#125) is the Fildes Peninsula, a foreland in the south-western end of King George Island, in the South Shetland Islands of Antarctica. One of the eight ASPA 125 sites is Collins Glacier (a.k.a. Bellingshausen), a glacial dome defining the ice-cover limit at the southern-most tip of the Fildes Peninsula, south of which ice-free lands extend. Collins Glacier is retreating upon the current rise of the atmospheric temperature (Lee et al., 2009; Monien et al., 2011), causing the increase of surficial runoff and the ground waterlogging as the ice melts. Erosive effects and chemical weathering impact the ground, and the filling of land holes with melting water result into glacial lakes. These lakes are the main sinks for water loading solutes and particulate material from the whole catchment area, constituting integrative pictures of the local biological, geochemical, and physical processes. The geochemical characterization of these

lakes is important for understanding the geophysical events and environmental processes taking place in this vulnerable ecosystem affected by thermal destabilization. The few geochemical studies in this region are restricted to investigations focused on rocks (Smellie et al., 1984; Machado et al., 2005) soils (Mendoça et al., 2013; Michel et al., 2014; Boy et al., 2016) or marine sediments (Monien et al., 2011), With the only existing on lacustrine sediments describing mineralogical and chemical aspects (Alfonso et al., 2015).

The present study addresses the biogeochemical characterization of recent sediments from five glacial lakes in the Fildes Peninsula by combining bulk geochemistry and mineralogy with the use of lipid biomarkers and (bulk and compound specific) stable isotopic analysis. The aim is to provide a geochemical background to reconstruct major sources, environmental conditions, and processes affecting the supply and burial of OM in the Fildes Lakes. This study contributes to understand biogeochemical processes affecting the delivery and burial of OM in lacustrine sediments from the Fildes Peninsula, setting the basis for understanding future (biological, ecological, and geochemical) alterations in this highly vulnerable system upon the current climate warming.

2. Materials and methods

2.1. Study area and sampling setting

The Fildes Peninsula is a 7 km long peninsula situated in the south-western end of King George Island (62°08′–62°14′S and 59°02′–58°51′W), in the South Shetland Archipelago, Antarctica (Fig. 1a–b). With an approximate surface of 1400 km^2 (Peter et al., 2008), it represents one of the largest ice-free areas in the maritime Antarctic region. The peninsula is bordered to the south by the Fildes Strait, to the south-east by the Maxwell Bay (a.k.a. Fildes Bay), and to the west by the Drake Pass (Fig. 1c). On its link on the northeast to the rest of King George Island, the peninsula is covered by the Collins Glacier. Geologically, the Fildes Peninsula is a tableland made up of old coastal landforms, with numerous rocky outcrops and an average height of 30 m above sea level (Antarctic Treaty Secretariat, 2009). Its bedrock is primarily basaltic, with volcanic intrusions and pyroclastic sediments (Xianshen and Xiaohan, 1990).

The Fildes Peninsula is the most extensively snow-free coastal area in summer on the island, most of which is permanently covered by ice. The peninsula ice-free zones have been occupied by glaciers until recent times, mostly since the last glacial maximum (87,000–15,000 yr BP), when gradual and rapid retreatment events alternated, such as the Fildes deglaciation between 6,000 and 4,000 yr BP (Barsh and Mausbacher, 1986), or the progressive retreatment since 1500 yr BP (Serrano-Cañadas, 2003). Since the late Holocene, the surviving ice cover (i.e. Collins Glacier) remains stable, with an estimated ice retraction of only a few tens of meters (Hall et al., 2010). The stability of the glacier is largely explained by its geographical location (inland) and dome-shaped structure, both protecting from marine wave action and climate fluctuations. Nevertheless, recent data suggest a continuous glacier retreatment during the last 30 years, due to the increase of mean annual air temperatures and the resulting liquid rain (Vieira et al., 2015).

Climate in the Fildes Peninsula is typically cold, moist maritime, with a mean annual temperature of −2.1 °C (Michel et al., 2012). In summer, mean daily temperature reach up to 2 to 3 °C, whereas in winter long-term monthly mean temperature can drop below −7 °C (Braun et al., 2004). The northern region of the peninsula is directly influenced by the Collins Glacier and contains abundant proglacial lakes (i.e. those formed by ice melting behind an ice dam or a moraine left by a retreating glacier; Embleton-Hamann, 2004), as well as recent glacial deposits. In contrast, the central and south region has been longer exposed, thus, less affected by glacial processes. Lakes in that region are rather periglacial (i.e. associated to frost action and/or permafrost related processes, when the natural drainage of the topography is obstructed by an ice sheet, ice cap or glacier; French, 2007), with
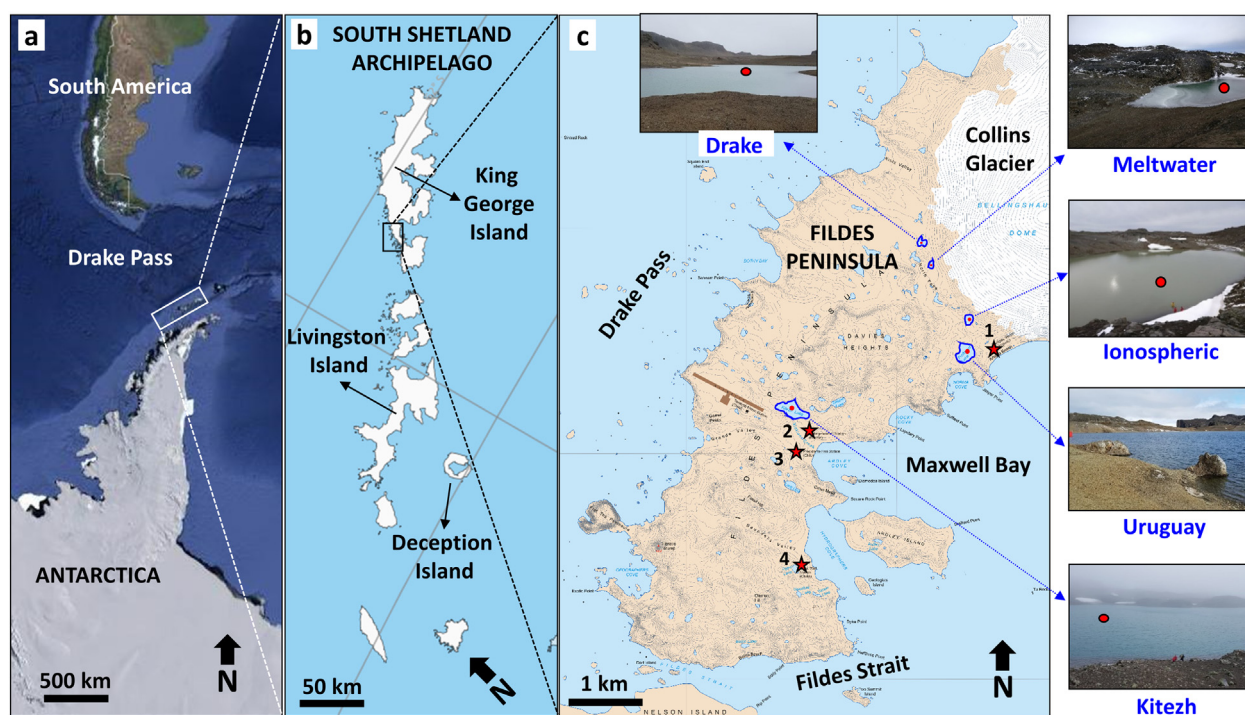
Fig. 1. Map of Antarctica (a), showing the South Shetland Archipelago (b), and a close-up of the Fildes Peninsula (c), where the five lakes were studied. Drake, Meltwater, Ionospheric, and Uruguay are classified as proglacial lakes, whereas Kitezh as periglacial (Vieira et al., 2015). Red stars in c indicate the location of the Antarctic scientific bases from Uruguay (1), Chile (2), Russia (3), and China (4). The Fildes Peninsula topographical map in c (1:25,000) was obtained from the Australian Antarctic Data Center (https://data.aad.gov.au/aadc/mapcat; Map Nr. 13799). (For interpretation of the references to color in this figure legend, the reader is referred to the web version of this article.)

influence of disturbing agents such as wind, snow melting, rain, or marine action.

Lichens and mosses are the dominant components of the terrestrial vegetation in the Fildes Peninsula as in the rest of Antarctica, with poorly developed tundra-like vegetation covering the foreland. One of the greatest diversity of mosses in Antarctica is on King George Island (i.e. 64 species), where the Fildes Peninsula is particularly rich due to the abundance of streams, pools and lakes providing the humid conditions needed by this flora (Li et al., 2009). *Deschampsia Antarctica* and *Colobanthus quitensis* are two species of higher plants described in Maritime Antarctica, where the Antarctic hairgrass *D. Antarctica* is extensively propagated over large areas including the Fildes Peninsula (Torres-Mellado et al., 2011), whereas *Colobanthus quitensis* has been recently recorded on soils from the Byers Peninsula, Livingston Island, on South Shetland Islands (Vera et al., 2013).

2.2. Sample collection

Surface sediments were sampled from different lakes on the Fildes Peninsula during a geochemical sampling campaign in February–March 2018, under the support of the Uruguayan IAU (Instituto Antártico Uruguayo) at the Artigas Base. Five lakes of different typology were sampled from the vicinity of the Collins Glacier at different locations; a few meters apart (90–210 m) from the glacier margin (Drake, Meltwater and Ionospheric lakes), or about 0.6 km (Uruguay) or 3.4 km (Kitezh) apart to the southwest (Table 1, Fig. 1c). The location of the lakes is shown in Fig. 1, and topographical and hydrographical features are summarized in Table 1. The Ionospheric, Kitezh, and (mostly) Uruguay lakes are located closer to the Maxwell Bay coastline relative to the other two lakes. Drake and Meltwater are the smallest (<3000 m²) and shallowest lakes (1–2 m depth), whereas Ionospheric, Uruguay, and Kitezh have larger (>16,200 m²) and deeper (10–15 m depth) watersheds (Table 1). Unlike all others, the Ionospheric Lake has a continuous inlet of water from the leaking Collins Glacier, and an outlet that discharges in the Maxwell Bay, both ensuring a regular

water turnover. In the five lakes, surface sediments (upper 3 cm depth) were collected from the deepest section of the lakes by a scuba diver using a stainless steel tube (30 cm depth and 66 mm i.d) as a dragging tool. The surface sediment samples (~30 g) were transferred to organics-free polyethylene containers with the aid of a solvent-clean (dichloromethane/methanol, 3:1) scoop, and then rapidly closed. Additionally, fresh samples representative of the local vegetation were collected from the lakes surroundings. One sample of moss (*Sanionia uncinata*), particularly abundant in the northern part of the Fildes Peninsula, was collected from the Drake and Meltwater surroundings;

Table 1
Geographical and geochemical features of the five Fildes lakes.

	Drake	Meltwater	Ionospheric	Uruguay	Kitezh
Latitude	62°10′16″	62°10′19″	62°10′48″	62°11′06″	62°11′36″
Longitude	58°55′37″	58°55′40″	58°54′39″	58°54′40″	58°57′58″
Altitude (m.a.s.l.)[a]	41	42	20	3	1
Lake area (m²)	2958	400	16,235	69,781	95,668
Lake maximum depth (m)	2	1	10	15	15
Distance to shoreline (m)	1523	1569	568	147	473
Distance to Collins Glacier ice margin (m)	92	120	215	624	3381
TOC (% dw)[b]	0.62	0.38	0.27	4.0	2.1
TN (% dw)[c]	0.06	0.03	0.03	0.26	0.17
C/N[d]	10	12	10	15	12
$\delta^{13}C$ (‰)	−20.7	−19.5	−23.4	−24.2	−23.4
$\delta^{15}N$ (‰)	−2.0	−0.2	−1.2	−1.4	1.3
Lake type[e]	Proglacial	Proglacial	Proglacial	Proglacial	Periglacial

[a] Meters above sea level.
[b] Total organic carbon, percentage relative to total dry weight.
[c] Total nitrogen, percentage relative to total dry weight.
[d] Ratio of TOC over TN (dimensionless).
[e] Classification based on Vieira et al. (2015).

two types of lichens (*Lecanora* spp., and *Placopsis contortuplicata*) from the region between the Ionospheric and Uruguay lakes; and one sample of grass (*Deschampsia Antarctica*) from the Kitezh surroundings. All sediment and vegetal samples were stored cold (~4 °C) on solvent-clean polypropylene containers until back at the laboratory, when they were frozen (−20 °C). They were then freeze-dried before geochemical analysis.

2.3. Mineralogy and geochemistry analysis

The five surface sediments were analyzed for mineral composition with a Bruker X-Ray diffractometer (AXS D8-Focus, XRD). The samples were scanned after drying and grinding in the 2·Θ-diffraction angle from 5° to 70°, with a scanning step size of 0.01°, at 40 kV and 40 mA with a Cu X-ray source (Cu Kα1,2, λ = 1.54056 Å).

Inorganic anions were determined by ion chromatography in the soluble phase of the sediment samples. This analysis is fully described elsewhere (Parro et al., 2011; Sánchez-García et al., 2018). Briefly, aliquots of 1 g of sample were sonicated (3 × 1 min cycles), diluted in 10 ml of deionized water, and filtered through a 22 μm GFF filter. The supernatants were collected and loaded into a Metrohm 861 Advanced compact ion chromatograph (Metrohm AG, Herisau, Switzerland). The column Metrosep A supp 7-250 was used with 3.6 mM sodium carbonate ($NaCO_3$) as eluent. Total major and minor elements were measured with Ion Coupled Plasma-Mass Spectrometry (ICP-MS). Microwave digestion using Teflon vessels were used according to previously described methods (Nna-Mvondo et al., 2008).

Stable isotope ratios of total organic carbon ($\delta^{13}C$) and total nitrogen ($\delta^{15}N$) were measured using isotope-ratio mass spectrometry (IRMS), and following the analytical methods by the USGS (Révész et al., 2012). Briefly, the sediment samples were homogenized using mortar and pestle. HCl (3 N) was added to the samples to remove carbonates, and, after equilibration for 24 h, adjusted to neutral pH with ultrapure water. The sample was oven dried (50 °C) until constant weight. Then, the $\delta^{13}C$ and $\delta^{15}N$ ratios were measured in a MAT 253 IRMS (Thermo Fisher Scientific) and reported in the standard per mil notation. Three certified standards (USGS41, IAEA-600, and USGS40) were used to report an analytical precision of 0.1‰. The content of total nitrogen (TN %) and total organic carbon (TOC %) was measured with an elemental analyzer (HT Flash, Thermo Fisher Scientific) during stable isotope measurements.

2.4. Lipid extraction, fractionation, analysis and QA/QC

Lyophilized subsamples of the lacustrine sediments (5–10 g) and vegetal materials (~0.5 g) were extracted with a mixture of dichloromethane/methanol (DCM/MeOH, 3:1, v/v) by ultrasound sonication following the method described elsewhere (Sánchez-García et al., 2018). Internal standards (tetracosane-D$_{50}$, myristic acid-D$_{27}$, and 2-hexadecanol) were added prior to extraction. The total lipid extracts (TLE) were concentrated to ~2 ml using rotary evaporation, and elemental sulfur was removed with activated cooper. The TLE was separated into neutral and acidic fractions using a Bond-elute column chromatography (bond phase NH$_2$, 500 mg, 40 μm particle size), by eluting with 15 ml DCM/2-propanol (2:1,v/v) and with 15 ml of acetic acid (2%) in diethyl ether, respectively. The neutral lipid fraction was then further separated into non-polar and polar fractions, by eluting on an alumina column (ca. 0.5 g of Al$_2$O$_3$ powder in a Pasteur pipet) with 4.5 ml of hexane/DCM (9:1, v/v) and 3 ml of DCM/methanol (1:1, v/v), respectively. The acidic fraction was derivatized with BF$_3$ in methanol and the polar fraction with N,O-bis (trimethylsilyl) trifuoroacetamide (BSTFA), respectively producing fatty acid methyl esters (FAME) and trimethylsilyl alcohol derivatives.

The three polarity fractions were analyzed by gas chromatography mass spectrometry using a 6850 GC system coupled to a 5975 VL MSD with a triple axis detector (Agilent Technologies) operating with electron ionization at 70 eV and scanning from *m/z* 50 to 650. The analytes were injected (1 μl) and separated on a HP-5MS column (30 m × 0.25 mm i.d. × 0.25 μm film thickness) using He as a carrier gas at 1.1 ml min^{-1}. For the non-polar fraction, the oven temperature was programmed from 50 °C to 130 °C at 20 °C min^{-1}, then to 300 °C at 6 °C min^{-1} (held 20 min). For the acidic fraction, the oven temperature was programmed from 70 °C to 130 °C at 20 °C min^{-1} and to 300 °C at 10 °C min^{-1} (held 10 min). For the polar fraction, the oven temperature program was the same as for the acidic fraction, but the oven was held for 15 min at 300 °C. The injector temperature was 290 °C, the transfer line was at 300 °C and the MS source at 240 °C. Compound identification was based on the comparison of mass spectra (NIST library) and/or the use of reference compounds, which were quantified using external calibration curves. External standards of *n*-alkanes (C$_{10}$ to C$_{40}$), FAME (C$_8$ to C$_{24}$), *n*-alcohols (C$_{10}$, C$_{14}$, C$_{16}$, C$_{18}$, C$_{20}$) and branched isoprenoids (pristane and phytane) were injected to obtain calibration curves. Sigma Aldrich supplied all pure chemicals and standards. The analytical series included two procedural blanks (solvents), which were processed and analyzed to verify method recovery and absence of undesired contamination. Limits of quantification (LOQ) for *n*-alkanes, *n*-alkanoic acids and *n*-alkanols were determined using the lowest point in the calibration curve; 0.3 ng·g^{-1} dw for *n*-alkanes, and 0.5 ng·g^{-1} dw for both *n*-alkanoic acids and *n*-alkanols. Recoveries of the internal standards averaged 75 ± 11%.

2.5. Compound specific isotope analysis

The compound-specific isotopic composition of carbon was measured on certain lipid families (*n*-alkanes and *n*-alkanoic acids as FAME). The compound-specific isotopic analysis (CSIA) was performed coupling the gas chromatograph (Trace GC 1310 ultra) to the isotope-ratio mass spectrometry system (MAT 253 IRMS, Thermo Fisher Scientific). The conditions for the GC analysis were identical to those set for the molecular analysis of the polar fraction, whereas those for the IRMS analysis were as follows: electron ionization 100 eV, Faraday cup collectors *m/z* 44, 45 and 46, and temperature of the CuO/NiO combustion interface of 1000 °C. The samples were injected in splitless mode, with an inlet temperature of 250 °C, and helium as a carrier gas at constant flow of 1.1 ml min^{-1}. Isotopic values of the individual lipids separated by GC were calculated using CO$_2$-spikes of known isotopic composition, introduced directly into the MS source, three times at the beginning and end of every run. Reference mixtures (Indiana University, USA) of known isotopic composition of *n*-alkanes (A6) and FAME (F8) were run every four samples to check accuracy of the isotopic ratio determined by the GC-IRMS. For the *n*-alkanoic acids, the $\delta^{13}C$ data were calculated from the FAME values, by correcting them for the one carbon atom added in the methanolysis (Abrajano et al., 1994).

2.6. Statistical analysis

A multivariate principal components analysis (PCA) was performed using the Infostat software version 2018 (Di Rienzo et al., 2018) to examine the relationship between the five lakes and certain biogeochemical variables. The PCA was based on a correlation matrix combining 10 standardized variables; TOC, TN, $\delta^{13}C$, $\delta^{15}N$, terrestrial sterols (i.e. sum of β-sitosterol, campesterol, or stigmasterol), brassicasterol, carbon preference index (CPI) of *n*-alkanes (C$_{20}$-C$_{31}$), high over middle-molecular weight *n*-alkanes (HMW/MMW), terrestrial over aquatic ratio of *n*-alkanes (TAR), as well as the pristane over phytane ratio (Pr/Ph).

3. Results

3.1. Mineralogical and geochemical composition of the surface sediments

XRD analysis identified the presence of plagioclases (anorthite and andesine), quartz, and pyroxenes in the surface sediments of the five

Table 2
Mineralogical composition (presence/absence) and concentration ($\mu g \cdot g^{-1}$) of inorganic and organic anions, as well as major and minor elements, in the surficial sediment samples from the five Fildes lakes.

Mineralogy (presence/absence)	Drake	Meltwater	Ionospheric	Uruguay	Kitezh
Plagioclases	x	x	x	x	x
Quartz	x	x	x	x	x
Pyroxenes	x	x	x	x	x
Zeolites				x	x
Clays				x	x
Anions ($\mu g \cdot g^{-1}$)	**Drake**	**Meltwater**	**Ionospheric**	**Uruguay**	**Kitezh**
Sulfate	23	153	10	1632	430
Chloride	0.47	14	2.8	49	63
Nitrate	n.d.	n.d.	0.47	1.06	n.d.
Bromide	n.d.	n.d.	n.d.	0.32	n.d.
Fluoride	n.d.	0.35	0.12	n.d.	0.39
Major and minor elements ($\mu g \cdot g^{-1}$)	**Drake**	**Meltwater**	**Ionospheric**	**Uruguay**	**Kitezh**
Na	81	95	34	27	29
Mg	9.5	16	5.8	2.0	3.3
Ca	11	19	7.5	2.0	5.5
Si	4.5	4.4	3.0	7.0	6.7
K	2.6	2.7	1.3	1.5	1.5
Al	0.10	0.06	0.70	1.5	1.0
S	5.2	36	14	4.0	7.0
Fe	0.10	0.14	0.20	1.0	0.10
Ti	0.01	0.004	0.04	0.10	0.07

x means presence, and n.d. not detected.

lakes, whereas zeolites (montmorillonite) and clays (kaolinites) were only observed in the Uruguay and Kitezh lakes (Table 2).

Ion chromatography analysis determined a variable concentration of inorganic anions among the lakes (Table 2). Sulfate and chloride were detected in the five sediments, the former at concentration one or two orders of magnitude larger (10–1632 $\mu g \cdot g^{-1}$) than the latter (0.47–63 $\mu g \cdot g^{-1}$). Uruguay and Kitezh were the lakes containing larger amounts of both anions. Nitrate, bromide and fluoride were only detected in some of the lakes at concentrations close to or lower than 1 $\mu g \cdot g^{-1}$ (Table 2). Neither nitrite nor phosphate was detected in the Fildes sediments.

ICP-MS determined the concentration of the major and minor elements showing different trends (Table 2), where the Drake, Meltwater and Ionospheric lakes generally showed larger concentration of Na, Mg, and Ca, whereas Uruguay and Kitezh of Si, Al or Ti.

The TOC content was measured to vary from 0.27% in the Ionospheric to 4.0% in the Uruguay Lake (Fig. 2a), relative to dry weight (% dw).

Similarly, the lowest concentration of TN was found in the sediments from the Ionospheric and Meltwater lakes (0.03%) and the largest in the Uruguay Lake (0.26%) (Table 1). The Uruguay and Kitezh surface sediments contained an order of magnitude larger TOC and TN than the other three lakes. The TOC over TN ratio (C/N) ranged among the five lakes from 10 to 15 (Fig. 2b). The organic carbon $\delta^{13}C$ ratio was measured to vary from −24.2‰ (Uruguay) to −19.5‰ (Meltwater), while the total nitrogen $\delta^{15}N$ from −2.0‰ (Meltwater) to 1.3‰ (Kitezh). For the fresh vegetal material, the stable isotopic analysis on the bulk biomass produced $\delta^{13}C$ values from −29.2 to −22.3‰ (lichens), of −27.2‰ (moss), and − 28.6‰ (grass), and $\delta^{15}N$ ratios from −2.2 to −1.6‰ (lichens), −2.0‰ (moss) and 8.2‰ (grass).

3.2. Lipid biomarkers in the Fildes Lakes surface sediments

The GC–MS analysis of the lipid extracts detected the presence of diverse lipidic families (n-alkanes, n-alkanoic acids, n-alkanols, isoprenoids, and sterols) in the five surface sediments. n-Alkanes were found to be present in total concentrations ranging from 0.29 to 1.5 $\mu g \cdot g^{-1}$ of TOC (Table 3). The sediments from Kitezh showed the largest amount of n-alkanes, whereas those from the other four lakes varied little between each other. This family was composed of linear and saturated alkanes (i.e. n-alkanes) between C_{12} and C_{31}, with a general dominance of the odd-numbered homologues. The five n-alkanes profiles (Fig. S1) showed a similar pattern with maxima at either C_{27}, C_{29} or C_{31}, and minor additional peaks at C_{23} (Drake, Ionospheric and Kitezh), C_{23} and C_{25} (Meltwater), or C_{21} (Uruguay). The average chain length (ACL) of the n-alkanes was virtually the same (i.e. 25) in the five sediments (Table 3), whereas the carbon preference index (CPI) ranged from 1.3 to 4.5 (Table 3). Source-diagnosis n-alkanes ratios varied from 4.6 to 30 (terrigenous over aquatic ratio or TAR), from 1.1 to 4.4 (high- over mid-molecular weight n-alkanes or $[HMW/MMW]_{n\text{-alkanes}}$), or from 0.23 to 0.61 ($Paq = [C_{23} + C_{25}] / [C_{23} + C_{25} + C_{29} + C_{31}]$; Figs. 3 and 4; see Table 3 for ratios definition).

Together with the n-alkanes, the isoprenoids pristane and phytane were also found in the five surface sediments, at concentrations ranging from 0.003 to 0.09 $\mu g \cdot g^{-1}$ of TOC (Table 3). The ratio of pristane over phytane (Pr/Ph) was higher in Drake, Meltwater, and Ionospheric (5.3–8.4) than in Kitezh and, mostly, Uruguay (Fig. 3c).

The acidic fraction was observed to contain n-alkanoic acids from C_{10} to C_{30} (Fig. S2), at total concentrations ranging from 1.9 $\mu g \cdot g^{-1}$ (Uruguay) to 38 $\mu g \cdot g^{-1}$ of TOC (Meltwater). Within this family, the even dominated over the odd n-alkanoic acids, with maximum peaks at C_{24}, C_{26} or C_{28} (Fig. S2). The ACL of the n-alkanoic acids ranged from 21 to 25 (Table 3).

The polar fraction contained an n-alkanols homologous series spanning from C_{10} to C_{30}, with dominance of the even compounds
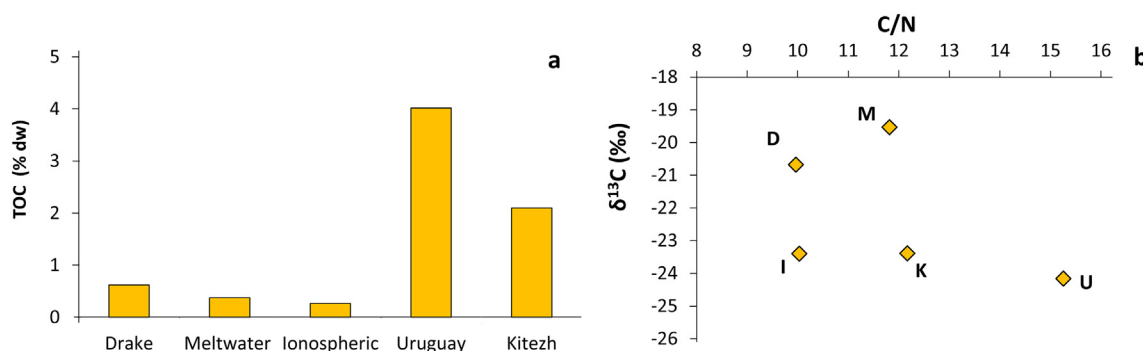

Fig. 2. Geochemical composition of the bulk organic fraction in the surface sediments from the five Fildes Lakes; (a) concentration of total organic carbon (% relative to the total dry weight) and (b) C/N ratios versus stable carbon isotopic composition of organic carbon (‰ PDB). The five lakes are identified by their initials in panel b.

(Fig. S3). The *n*-alkanols were measured at total concentrations from 0.13 $\mu g \cdot g^{-1}$ (Kitezh) to 3.2 $\mu g \cdot g^{-1}$ of TOC (Meltwater). The largest content of *n*-alkanols was found in the surface sediments from the Meltwater (maximum at C_{26}) and Uruguay (maximum at C_{22}) lakes (Table 3). The *n*-alkanol ACL varied from 19 to 24, and the TAR from 0.38 to 15 (Table 3). Phytol was also detected within the polar fraction at concentrations ranging from 0.02 to 0.11 $\mu g \cdot g^{-1}$ of TOC, together with a series of sterols (β-sitosterol, campesterol, brassicasterol and stigmasterol) of individual concentrations ≤0.21 $\mu g \cdot g^{-1}$ of TOC (Table 3). Meltwater showed the largest concentration of β-sitosterol (0.21 $\mu g \cdot g^{-1}$ of TOC), Drake and Meltwater that of brassicasterol (0.09 and 0.08 $\mu g \cdot g^{-1}$ of TOC, respectively), and Uruguay of campesterol (0.13 $\mu g \cdot g^{-1}$ of TOC) (Table 3).

The fresh vegetal samples contained *n*-alkanes spanning from C_{11} to C_{32} with variable profiles depending on the particular species (Fig. S4). The moss sample (*Sanionia unciata*) exhibited a distinct maximum at C_{23}. The Antarctic grass (*Deschampsia antarctica*) had its maximum at C_{31}, with relevant peaks also at C_{23} and C_{25}. The two lichen samples (*Placopsis contortuplicata* and *Lecanora* sp.) showed a common maximum at C_{17}, and additional peaks at C_{21}, C_{22}, C_{23}, or C_{27} (Fig. S4).

Table 3
Concentration ($\mu g \cdot gOC^{-1}$) and compositional distribution of lipid biomarkers in the five lacustrine sediments.

	Drake	Meltwater	Ionospheric	Uruguay	Kitezh
n-Alkanes	0.33	0.40	0.48	0.29	1.5
ACL *n*-alkanes (C_{10}-C_{31})[a]	25	25	25	25	25
CPI *n*-alkanes (C_{20}-C_{31})[b]	1.3	2.5	1.4	4.5	2.8
HMW *n*-alkanes[c]	0.27	0.37	0.41	0.27	1.38
HMW/MMW *n*-alkanes[d]	1.6	1.7	1.1	3.4	4.4
TAR *n*-alkanes[e]	4.6	29	9.7	23	30
Paq[f]	0.49	0.49	0.61	0.33	0.23
Sum of ($C_{27} + C_{29} + C_{31}$)	0.09	0.15	0.11	0.14	0.76
Pristane	0.09	0.02	0.02	0.02	0.02
Phytane	0.01	0.004	0.003	0.03	0.01
Pr/Ph	8.4	5.3	5.5	0.62	1.9
n-Alkanoic acids	2.9	38	8.1	1.9	2.5
ACL *n*-alkanoic acids (C_{10}-C_{30})[a]	22	24	21	25	23
HMW *n*-alkanoic acids	1.9	32	4.5	1.7	1.7
TAR *n*-alkanoic acids[g]	2.5	9.2	1.7	17	3.9
Sum of ($C_{24} + C_{26} + C_{28}$)	1.1	21	2.8	1.0	1.2
n-Alkanols	0.36	3.2	0.15	1.9	0.13
ACL *n*-alkanol (C_{10}-C_{30})[a]	23	24	19	23	21
HMW *n*-alkanols[c]	0.28	2.9	0.06	1.7	0.08
Sum of ($C_{26} + C_{28} + C_{30}$)	0.06	0.66	0.005	0.19	0.01
TAR *n*-alkanols[h]	3.2	15	0.38	9.2	1.1
Phytol	0.02	0.06	0.02	0.11	0.01
β-Sitosterol[i]	0.13	0.21	0.07	0.18	0.02
Campesterol[j]	0.07	0.10	0.03	0.13	n.d.
Stigmasterol[k]	0.03	0.06	0.01	0.11	0.01
Brassicasterol[l]	0.09	0.08	0.02	0.05	n.d.

[a] ACL$_{i-n}$ average chain length = $\sum (i \cdot X_i + ... + n \cdot X_n) / \sum X_i + ... + X_n)$, where X is concentration (van Dongen et al., 2008).

[b] CPI$_{i-n}$, carbon preference index = $\frac{1}{2} \sum (X_i + X_{i+2} + ... + X_n) / \sum (X_{i-1} + X_{i+1} + ... + X_{n-1}) + 1/2 \sum (X_i + X_{i+2} + ... + X_n) / \sum (X_{i+1} + X_{i+3} + ... + X_{n+1})$, where X is concentration (van Dongen et al., 2008).

[c] High molecular weight *n*-alkanes, *n*-alkanoic acids or *n*-alkanols, sum of the concentrations of homologues ≥C_{21}.

[d] High over mid-molecular weight *n*-alkanes = ($C_{27} + C_{29} + C_{31}$) / ($C_{23} + C_{25}$).

[e] Ratio of terrigenous over aquatic *n*-alkanes = ($C_{27} + C_{29} + C_{31}$) / ($C_{17} + C_{19}$) (van Dongen et al., 2008).

[f] P$_{aq}$, ratio of emergent and submerged over floating macrophytes = ($C_{23} + C_{25}$) / ($C_{23} + C_{25} + C_{29} + C_{31}$) (Ficken et al., 2000).

[g] Ratio of terrigenous over aquatic *n*-alkanoic acids = ($C_{24} + C_{26} + C_{28}$) / ($C_{14} + C_{16} + C_{18}$) (van Dongen et al., 2008).

[h] Ratio of terrigenous over aquatic *n*-alkanols = ($C_{26} + C_{28}$) / ($C_{16} + C_{18}$) (van Dongen et al., 2008).

[i] β-Sitosterol, 24-ethyl-cholest-5-en-3β-ol.

[j] Campesterol, 24-methylcholest-5-en-3β-ol.

[k] Stigmasterol, 24-ethylcholest-5,22E-dien-3β-ol.

[l] Brassicasterol, 24-methyl cholest-5,22-dien-3β-ol.

The fresh samples produced P$_{aq}$ ratios between 0.53 (grass) and 1.0, and CPI values between 0.94 and 5.8 (Fig. 4).

3.3. Compound specific isotope analysis of lipids biomarkers

The compound-specific isotopic composition of the sedimentary *n*-alkanes varied widely (from −23.7 to −39.6‰) between the Fildes lakes (Table S4). In general, the variation of $\delta^{13}C$ was greater within the LMW and MMW *n*-alkanes (from −23.7 to −39.6‰), than within those of HMW (from −27.2 to −33.1‰). Among the lakes, Drake and Ionospheric showed more homogeneous $\delta^{13}C_{n-alkanes}$ ratios than Meltwater, Uruguay and Kitezh. Sediments from the two latter lakes had the most $\delta^{13}C$-depleted *n*-alkanes, namely, C_{19} in Uruguay and C_{21} in Uruguay and Kitezh (Fig. 5), whereas Meltwater contained the most $\delta^{13}C$-enriched alkanes (i.e. C_{23} and C_{25}) together with Kitezh (C_{17}). The $\delta^{13}C$ ratios varied less for the *n*-alkanoic acids (from −21.0 to −31.7‰). In the five lakes, the LMW *n*-alkanoic acids (C_{14}, C_{16}, and C_{18}) showed relatively enriched $\delta^{13}C$ ratios (from −22.6 to −24.7‰), whereas those of HMW (C_{24}, C_{26}, and C_{28}) were generally ^{13}C-depleted (from −21.0 to −31.7‰), except for the Meltwater sediments (Fig. 6).

3.4. PCA analysis

The multivariate PCA produced a separation of the Fildes Lakes into two groups according to the geochemical composition of their surface sediments; Uruguay and Kitezh (group I), versus Drake, Ionospheric and Meltwater (group II). Two principal components were extracted from the multivariate analysis that accounted together for 79.6% of the total variance (Fig. 7). The first principal component (PC1) explained 56.0% of the variance, and the second (PC2) contributed 23.6%. Taking into account the eigenvectors magnitude, the most important parameters on the PC1 are the Pr/Ph ratio, TN, TOC, CPI of *n*-alkanes, and Paq. Pr/Ph and P$_{aq}$ are strongly and positively correlated between them and, to a lesser extent, with $\delta^{13}C$, but negatively correlated with TN, TOC, CPI of *n*-alkanes, and TAR (Table S5). As for the PC2, the most important contributors are the sum of terrestrial sterols, brassicasterol and $\delta^{15}N$ (Fig. 7), which are negatively correlated (Table S5).

4. Discussion

4.1. Heterogeneous carbon sources in the surface sediments from the Fildes Lakes

Elemental, isotopic and molecular biomarkers show quantitative and qualitative differences in the composition of their sedimentary OM in the five Fildes Lakes. The deepest lakes (i.e. Uruguay and Kitezh), contain the OM-richest sediments (i.e. highest TOC and TN) and relatively depleted $\delta^{13}C$ values (Fig. 2), characteristic of lacustrine environments. Stable carbon isotopic signatures are commonly used to investigate sources of OM, where terrestrial carbon sources (i.e. higher plants using the C3 pathway) generally have $\delta^{13}C$ values around −27‰, aquatic carbon sources (i.e. phytoplankton and algae) typical values around −21‰ (Fry and Sherr, 1984; Meyers, 1994), and mosses around −23‰ (Boy et al., 2016). In the Fildes Peninsula, the intermediate $\delta^{13}C$ values in the Uruguay (−24.2‰), Kitezh (−23.4‰), and Ionospheric (−23.4‰) lakes suggest a relevant contribution from terrestrial carbon sources and are in the range of those measured in soil samples (from −22.3 to −25.6‰) collected from a glacier retreat gradient on the Fildes Peninsula *Meseta* (Boy et al., 2016), extensively covered by mosses, lichens and hairgrass. In contrast, the ^{13}C-enriched ratios in the OM-poorer Drake and Meltwater sediments (−20.7 and −19.5‰, respectively) reveal a relatively greater input from aquatic carbon sources. In the five lakes, C/N ratios ≥10 (Fig. 2b) are in the range of those typical of lacustrine sediments that is, between values typical from algae (4–10) and vascular plants (≥20) (Prahl et al., 1980;
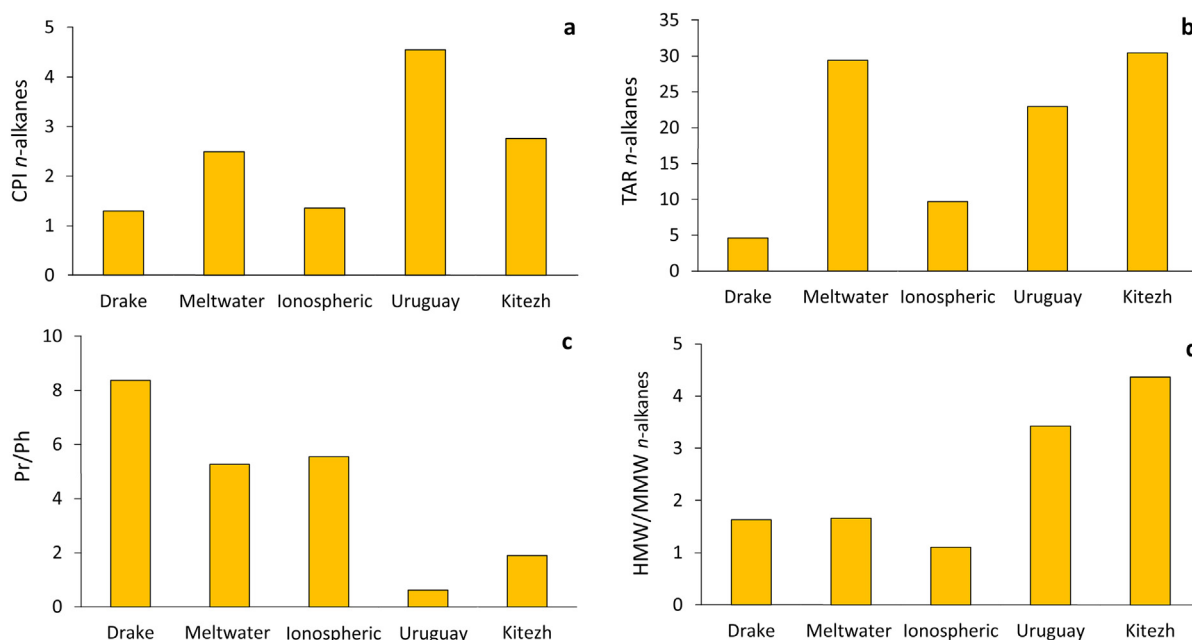
Fig. 3. Lipid proxies diagnostic of the origin of organic matter (OM) and the environmental conditions in the five surface sediments; a) carbon preference index of *n*-alkanes (biogenic vs. petrogenic origin), b) ratio of terrestrial over aquatic *n*-alkanes (terrestrial vs. aquatic OM origin), c) pristane over phytane ratio (oxic vs. anoxic conditions), and d) ratio of high molecular-weight over medium molecular-weight *n*-alkanes (relative abundance of higher plants vs. other type of vegetation). Please go to Table 2 for details on the ratios calculations.

Meyers, 1994). Bulk $\delta^{15}N$ ratios slightly higher or lower than zero (i.e. -2.0 to 1.3‰) indicate the participation of N_2-fixation sources (Robinson, 2001) such as land plants, algae, and/or cyanobacteria to the sediments of the five lakes. Both bulk-element and isotopic composition suggest a miscellaneous aquatic-terrestrial origin of the organic carbon in the surface sediments from the five Fildes Lakes.

Lipid distribution patterns and biomarkers proxies provide additional insights on the contribution from different carbon sources to sedimentary OM. In the Fildes Lakes, terrestrial sterols such as β-sitosterol, campesterol, or stigmasterol (Table 3) are ubiquitously detected in the five surface sediments. Consistently, molecular distribution patterns in *n*-alkanes, *n*-alkanoic acids, and *n*-alkanols reveal dominance of HMW moieties (i.e. ACL of 25, 21–24, and 19–24, respectively). HMW lipids of odd-over-even (*n*-alkanes) or even-over-odd (*n*-alkanoic acids and *n*-alkanols) predominance are typical for terrestrial plants (Eglinton and Hamilton, 1967; Hedges and Prahl, 1993). *n*-Alkanes distributions similarly dominated by odd HMW moieties (i.e., *n*-C_{25}, *n*-C_{27}, *n*-C_{29}, and *n*-C_{31}) have been also described in soil samples from four nearby

islands belonging to the South Shetland archipelago (Livingston, Deception, Penguin, and Barrientos), where Cabrerizo et al. (2016) explained those biogenic signals in relation to the general presence of mosses and vascular plants (grass and Antarctic pearlwort). The total concentration of *n*-alkanes in the surface sediments of the Fildes Lakes (0.29–$1.5 \, \mu g \cdot gOC^{-1}$ or 129–$3150 \, ng \cdot gdw^{-1}$) were in the range of those reported in soil samples from the South Shetland Islands (7–$3310 \, ng \cdot gdw^{-1}$; Cabrerizo et al., 2016) or from the McMurdo Dry Valleys of Southern Victoria Land (13–$2200 \, ng \cdot gdw^{-1}$), in the Antarctic continent (Matsumoto et al., 1990). In addition, the abundance of LMW *n*-alkanoic acids ($\leq C_{20}$) in the Meltwater and Ionospheric sediments (Fig. S2) relative to the other lakes suggests certain aquatic origin of the sedimentary OM in those lakes. Brassicasterol, a sterol commonly used as biomarker for freshwater and marine diatoms (e.g. Robinson et al., 1984; Yunker et al., 1995) is present in all lakes except Kitezh, although at larger concentration in Drake and Meltwater (Table 3). Still, TAR ratios higher than the unit (Table 3) are observed in all five sediments, pointing to the dominance of terrestrial over aquatic sources
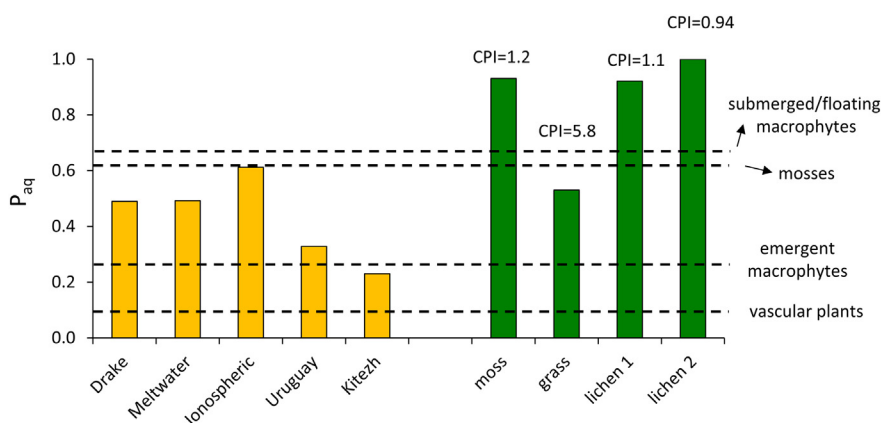

Fig. 4. *n*-Alkane proxy P_{aq} indicating the type of terrestrial sources in the surface sediments from the five Fildes Lakes and in fresh vegetal material from the surroundings. P_{aq} end-member ratios (dotted lines) from Ficken et al. (2000), Nott et al. (2000), Mead et al. (2005).
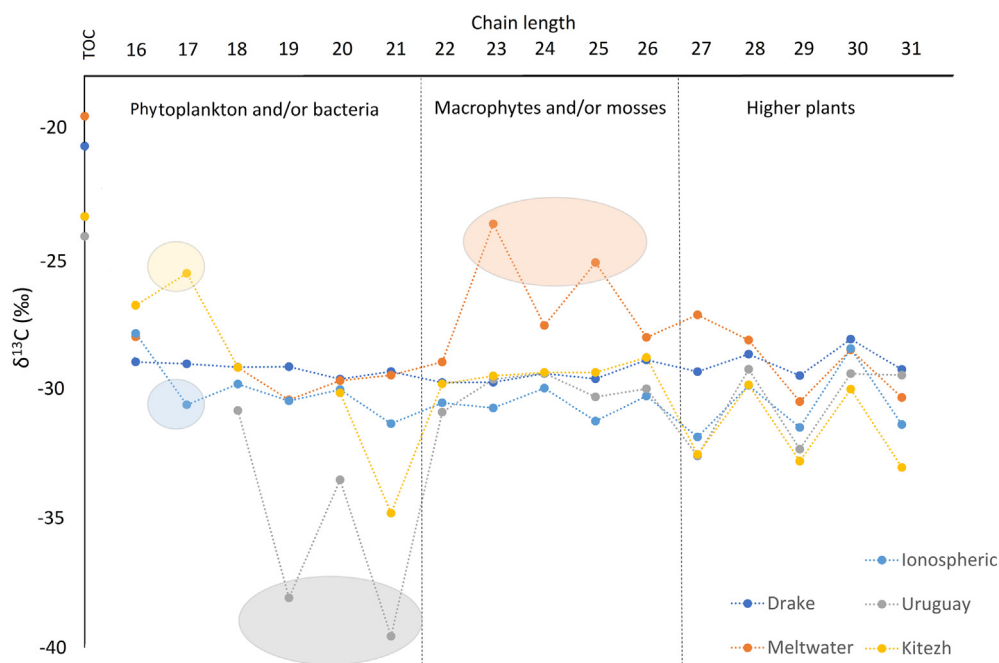
Fig. 5. Compound-specific isotopic composition (δ^{13}C) of *n*-alkanes in the surface sediments from the five Fildes lakes. Vertical dashed lines divide the distribution of *n*-alkanes (low, middle, or high molecular weight) according to characteristic organic-matter sources, that is, phytoplankton and/or bacteria, macrophytes and/or mosses, or higher plants, respectively (Eglinton and Hamilton, 1967; Fahl and Stein, 1997; Ficken et al., 2000). Particularly diverging δ^{13}C values are highlighted with colored ellipses in the Meltwater (δ^{13}C enriched C_{23} and C_{25}; orange), Ionospheric (δ^{13}C depleted C_{17}: blue), Uruguay (very δ^{13}C depleted C_{19} and C_{21}; blue), and Kitezh (δ^{13}C-enriched C_{17}; yellow) lakes. (For interpretation of the references to color in this figure legend, the reader is referred to the web version of this article.)

particularly in the Kitezh, Uruguay, and Meltwater lakes (Fig. 3b). In Kitezh and Uruguay, the elevated TAR values coincide with the depleted δ^{13}C (Fig. 2) and low P_{aq} ratios (Fig. 4). The alkane P_{aq} ratio (Table 3) is a proxy used to distinguish between different groups of aquatic versus land plants (Ficken et al., 2000; Mead et al., 2005), where land plants typically produce proxy values of 0.09, emergent macrophytes of 0.25, mosses around 0.63 (Nott et al., 2000), and submerged/floating macrophytes of 0.69 (Ficken et al., 2000). However, certain vascular plants may produce P_{aq} values >0.09, such as the grass *Deschampsia antarctica*, which was measured here to produce a P_{aq} of 0.53 or in the South Shetland Islands in the range from 0.57 to 0.61, as estimated from

their *n*-alkanes distributions (Cabrerizo et al., 2016). Other Antarctica vegetation such as the moss *Sanionia uncinata* has been measured to produce P_{aq} values varying from lower values (0.13–0.52) on the South Shetland Islands (Cabrerizo et al., 2016) to a larger value (0.93) in the Fildes Peninsula (Fig. 4). P_{aq} values in Antarctica lichens may also vary from 0.24 to 0.42 (*Usnea Antarctica* in the South Shetland Islands; Cabrerizo et al., 2016) to 0.92–1.0 (*Placopsis contortuplicata* and *Lecanora* sp., this study). Thus, the range of P_{aq} found in the surface sediments from the Fildes Lakes (0.23–0.61) suggests a mixed
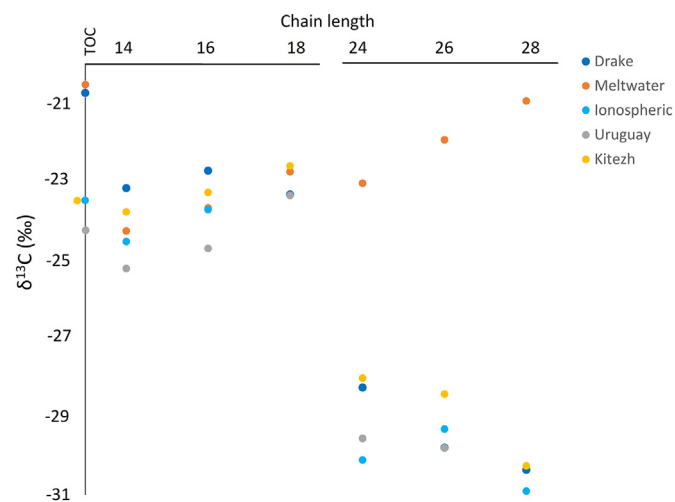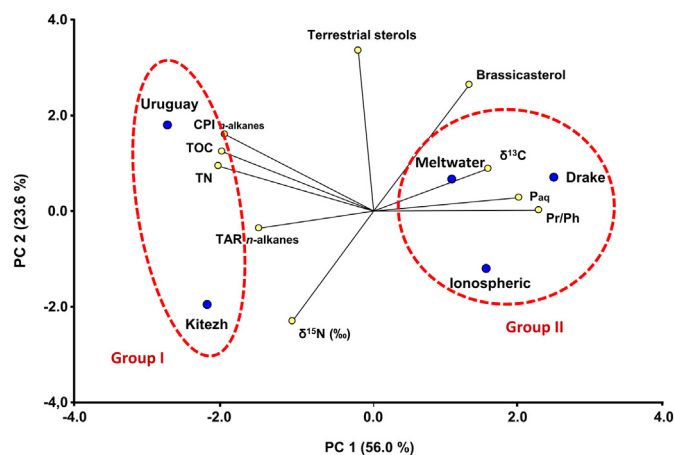

Fig. 7. Biplot diagram of the principal component analysis (PCA) for the five surface sediments and 10 variables studied; TOC, TN, δ^{13}C, δ^{15}N, terrestrial sterols (i.e., sum of β-sitosterol, campesterol, or stigmasterol), brassicasterol, CPI of *n*-alkanes, TAR$_{n\text{-alkanes}}$, P_{aq}, and Pr/Ph. Please see Table 2 for details on the ratios calculation. PC 1 and PC 2 explain together 79.6% of the system variance. The five sediment samples are represented as blue dots and the geochemical variables as yellow dots with vectors showing the variable direction. The loadings (displayed as correlation coefficients) on PC1 and PC2 are shown in Table S5. (For interpretation of the references to color in this figure legend, the reader is referred to the web version of this article.)

Fig. 6. Compound-specific isotopic composition (δ^{13}C) of source-diagnosis *n*-alkanoic acids in the five lacustrine sediments. To facilitate visualization, two separate plots are used to display the δ^{13}C composition of a) low molecular-weight congeners related to prokaryotic sources (C_{14}, C_{16} and C_{18}), and b) high molecular-weight acids typically produced by higher plants (C_{24}, C_{26}, and C_{28}).

contribution from emergent macrophytes, mosses, and vascular plants (Fig. 4). The higher P_{aq} values in the Drake, Meltwater, and Ionospheric sediments denote larger contribution from mosses and lichens, whereas the lower values in Uruguay and Kitezh reflect greater input from emergent macrophytes and/or grass. The difference of P_{aq} signatures in the Drake, Meltwater, and Ionospheric lakes versus (mostly) Kitezh may be related to the greater ground humidity in the northern lands close to the retreating Collins Glacier, where mosses and swamp vegetation find optimum conditions to grow.

The CPI values reveal qualitative differences on the sedimentary OM from the five Fildes Lakes. CPI is a proxy broadly used to distinguish between biogenic and petrogenic sources of hydrocarbons (Harrison, 2007), where recent biogenically derived n-alkanes (e.g. plants or biota exudates) tend to favor odd-carbon numbered chain lengths, whereas aged organic material such as petrogenic (i.e. rock-derived) hydrocarbons that have undergone ageing over geological timescales generally do not exhibit this odd-carbon number preference due to random cleavage of alkyl chains (Killops and Killops, 2005). Therefore, environmental samples with a CPI > 1 suggest that the aliphatic hydrocarbons have arisen thorough biogenic input (Rieley et al., 1991; Hedges and Prahl, 1993), whereas CPI values approaching 1 indicates petrogenic sources (Harrison, 2007). The CPI values in the surface sediments from the five Fildes Lakes (1.3–4.5) denote a general biogenic origin of the sedimentary organic carbon. Indeed the fresh moss, grass and lichen samples showed CPI values similarly varying from 0.94 to 5.8 (Fig. 4), consistent with CPI values reported on identical or similar vegetation species on the South Shetland Islands (Cabrerizo et al., 2016) calculated from a slightly different range of carbon units (C_{23}-C_{31}, rather than our C_{21}-C_{31}). CPI values similar to those measured in the Fildes sediments were observed in soil samples from the South Shetland Islands (i.e., 1.4–3.4; Cabrerizo et al., 2016) and the Antarctic McMurdo Dry Valleys (i.e., 1.98–2.59; Matsumoto et al., 2010) and attributed to lichens and/or vascular plant debris. However, in addition to the dominant biogenic origin, of certain input of petrogenic carbon cannot be ruled out in the Fildes Lakes, mostly in the Drake and Ionospheric sediments, where the lowest CPI values (i.e., 1.3 and 1.4, respectively) were measured (Fig. 3a). Similarly low CPI values (<1.5) in Antarctic settings on King George Island (Prus et al., 2015) or South Shetland Islands (Cabrerizo et al., 2016) were attributed to anthropogenic impacts related to proximity to polar scientific stations (e.g. fossil fuel combustion or oil spills from ships operations). Although such a contamination factor cannot be completely excluded in the Ionospheric Lake, given the relative proximity to the Uruguayan scientific station (Fig. 1), the fact that the lowest CPI value is found on the furthest lake to scientific polar stations, whereas the two lakes closest to them (i.e., Uruguay and Kitezh; Fig. 1) show the highest CPI values, suggest there must be other factors than anthropogenic explaining the petrogenic signature observed. Petrogenic (i.e. rock-derived) hydrocarbons in the Drake and Ionospheric lakes may rather come from physical erosion of bedrock (Galy et al., 2015). Given the proximity of the two lakes to the retreating Collins Glacier, we hypothesize that ancient carbon may be released from recently exposed surfaces of bedrock where erosion-protective vegetation has not yet developed as in longer-exposed further to the southwest. In addition, the low CPI values in the northern lakes may also denote certain contribution from bacterial sources, where microbial degradation would result into OM with lack of carbon-number preference (Killops and Killops, 2005). In glacial environments, ice is colonized by microbial organisms adapted to live in such cold conditions (e.g., chemoheterotrophs, anaerobic nitrate reducers, sulfate reducers or methanogens) (Skidmore et al., 2000), and sometimes it is covered by thin layers of wind-transported dark powdered material mainly composed by microbial derivate compounds called *cryoconite* (Xu et al., 2010). Upon melting, the glacial ice constitutes a potential source of microbial OM to the surrounding lakes (Skidmore et al., 2000).

The compound-specific isotopic composition (δ^{13}C) of n-alkanes and n-alkanoic acids also reveal qualitative differences in the molecular composition of the five lacustrine sediments. Overall, all n-alkanes (Fig. 5) and the HMW n-alkanoic acids (Fig. 6) show δ^{13}C ratios relatively depleted relative to the bulk OM (i.e. $\Delta\delta^{13}$C = 5–13‰) as typically observed on mixed lacustrine pools (Meyers, 1997). In the Drake and Ionospheric lakes, all n-alkanes display δ^{13}C values varying little between each other (2–4‰), in contrast to the other lakes showing δ^{13}C variations up to 10‰ (Fig. 5). For instance, in Uruguay and Kitezh certain LMW n-alkanes (i.e. C_{19} and C_{21}) are particularly ^{13}C-depleted (i.e. more negative δ^{13}C) relative to their homologues. The δ^{13}C depletion in the typically phytoplanktonic n-alkanes C_{19} and C_{21} (Thiel et al., 1997; Allen et al., 2010) may reflect trophic differences in the phytoplankton population of Uruguay and Kitezh relative to the other lakes. In aquatic systems with low primary productivity (i.e. oligotrophic), competition for carbon is low, therefore primary producers tend to discriminate against the heavier isotope (i.e. ^{13}C), thus resulting in more negative δ^{13}C values (Hollander and McKenzie, 1991). According to the TAR values, the weight of aquatic carbon sources in Uruguay, Kitezh, and Meltwater is lower than in the other two lakes. In Uruguay and Kitezh in particular, this coincides with their greater depth (i.e. 15 m) that typically hinders water mixing. Low availability of nutrients in poorly mixed, deep water columns and a lesser abundance of primary producers (i.e. oligotrophic conditions) may have caused a lower competition for carbon in the Uruguay and Kitezh lakes, thus resulting in the more negative δ^{13}C values of the planktonic C_{19} and C_{21} n-alkanes. In Meltwater in contrast, the MMW n-alkanes C_{23} and C_{25} display δ^{13}C values relatively enriched (~2–4‰) compared to the rest of n-alkanes (Fig. 5). This ^{13}C enrichment in n-alkanes particularly abundant in the analyzed moss and grass samples (Fig. S4b) may reflect greater contribution of either type of vegetation to this lake. As the Drake and Ionospheric lakes, Meltwater is located in the surroundings of Collins Glacier, where melting streams fed vast extensions of swamp vegetation, including moss and grass. In such waterlogged ground, vegetation can uptake carbon from other sources than atmospheric CO_2 (e.g. dissolved inorganic carbon or (DIC) (Ficken et al., 2000). The use of a carbon source enriched in ^{13}C ($\delta^{13}C_{DIC}$ ~0‰) relative to CO_2 (δ^{13}C ~−8‰) may result into OM with less negative δ^{3}C values. The stronger moss signal (^{13}C-enriched C_{23} and C_{25}) in the Meltwater relative to Drake and Ionospheric lakes may be the result of the lower alteration of biomass upon rapid sinking in this extremely small and shallow lake (i.e. 400 m^2 and 1 m depth), thus promoting the preservation of original organic signatures in the sediments.

The CSIA of n-alkanoic acids provides further evidence of the mixed carbon origin in the surface sediments of the Fildes Lakes. Overall, LMW n-alkanoic acids majorly derived from algae such as C_{14}, C_{16} and C_{18} are observed to be ^{13}C enriched by 3–5‰ (Fig. 6), according to the major use of ^{13}C-enriched carbon by primary producers (Cranwell et al., 1987). In contrast, land plant-derived HMW n-alkanoic acids such as C_{24}, C_{26}, and C_{28} (Rieley et al., 1991) are relatively ^{13}C depleted in the surface sediments of all lakes but Meltwater (Fig. 6). The δ^{13}C duality generally observed in the Fildes Lakes illustrates the combined contribution from terrestrial and aquatic carbon sources to the surface sediments, whereas the peculiar ^{13}C enrichment of the HMW n-alkanoic acids in Meltwater supports the greater input of swamp vegetation using ^{13}C-enriched sources of carbon (i.e. DIC) to the sediments of this shallow lake.

4.2. Factors influencing the sedimentary organic matter composition in the five Fildes Lakes

The elemental, molecular, and isotopic results on the five sediment samples allow sorting the Fildes Lakes into two different groups (Fig. 7), according to their geochemical composition. The Uruguay and Kitezh lakes form Group I, which surface sediments are the OM richest (high TOC and TN) and freshest (high CPI), with organic carbon largely derived from terrestrial sources (i.e. high $TAR_{n-alkanes}$ and depleted bulk δ^{13}C). Sedimentary conditions in these two lakes appear to be more or less anoxic according to Pr/Ph ratios lower (Uruguay) or slightly higher

(Kitezh) than 1 (Fig. 3c). Pristane and phytane are photosynthetic biomarkers (Ishiwatari et al., 1999) majorly originated from phytol (Brocks and Summons, 2003), which tends to degrade to either pristane or phytane depending on conditions of abundance or absence of oxygen, respectively (Peters et al., 2005). The Pr/Ph ratio is commonly used for reconstructing paleoredox conditions in sedimentary environments on early diagenetic states (Blumenberg et al., 2012), where values lower than 1 denote anoxia. In the deepest watersheds of Uruguay and Kitezh, mixing along the water column is not favored, thus promoting anoxic conditions at the lower water layers and surface sediments, where OM relatively preserved (i.e. fresh) tends to accumulate. This explains the lower Pr/Ph ratios and greater CPI values observed in the surface sediments from Uruguay and Kitezh relative to the other lakes. The mineralogy of the sediments in those two lakes denotes certain alteration, as zeolites and clays were found together with the widespread basaltic materials (Table 2). The presence of secondary aluminous clay in the Uruguay and Kitezh sediments may be explained by the chemical weathering of the original basaltic bedrock, as previously described in lakes from the extreme southern part of the Fildes Peninsula in the region furthest from Collins Glacier (Alfonso et al., 2015). Furthermore, a marine fingerprint is observed in the sediments of these two lakes in form of relative abundance of sulfate and chloride anions (Table 2), likely transported from the coast by marine aerosols and seawater drops.

The Drake, Ionospheric, and Meltwater lakes comprise Group II, which sediments contain relatively less biomass (low TOC and TN) that is less fresh (lower CPI) and largely derived from swamp vegetation (high P_{aq}) and/or aquatic (low TAR; just Drake and Ionospheric) carbon sources. Pr/Ph ratios considerably larger than 1 denote a relatively greater abundance of oxygen in the water column of these three lakes compared with those from Group I (Fig. 3c). Oxic conditions are characteristic of well mixed waters. In the shallow Drake and Meltwater (2 and 1 m depth, respectively), high oxygen concentration is likely assured thanks to the mixing effect of the frequent and strong polar winds. In the Ionospheric Lake, the continuous water input from the leaking Collins Glacier and output to the Maxwell Bay likely favor the mixing and oxygenation of water in this deeper watershed (10 m depth). The low TOC and CPI values in the three lakes, together with the monotonous distribution of ^{13}C-depleted n-alkanes in Drake and Ionospheric suggest certain contribution of petrogenic carbon sources (Drenzek et al., 2007), likely linked to erosion of recently-exposed bedrock material (i.e. ancient carbon) and glacial meltwater supply (Hood et al., 2009). This is consistent with the fresh mineralogy (i.e., basaltic with absence of secondary aluminous clays) and relative abundance of Na, Mg, and Ca cations in the three lakes closest to Collins Glacier. The glacial outflow from the retreating glacier flushes water bearing thaw and eroded particulate material into the Drake, Ionospheric and Meltwater lakes, thus imprinting their sediments with a similar inorganic signature. Moreover, the continuous meltwater leaking enhances the ground humidity and waterlogging that provides the suitable edaphic conditions for the swamp vegetation to grow and expand nearby Collins Glacier. The relatively greater imprint from mosses in Meltwater may be the result of a concentration effect owed to the very small size of the lake.

In sum, mineralogical, inorganic, isotopic, and lipid biomarker proxies reveal compositional differences in the surface sediments from the five Fildes Lakes, where factors such as the distance to the glacial ice margin, the proximity to the coast, and the lake depth seem to play a key role in determining their geochemical signature.

4.3. Study limitations

The present biogeochemical study involves certain limitations (majorly related with the sampling strategy) that should be mentioned. For instance the sampling size; a larger number of subsamples per lake would be desirable for a better statistical representativity of the studied

area. However, logistical constrains and hard working conditions (i.e., highly variable meteorology, extremely cold water temperatures, diving time frames of 15–20 min maximum, sharing the scuba diver working time, campaign of fixed time-period, etc.) restricted our sampling capability to only one sample per lake. Counting on scuba divers with exclusive dedication to our project or longer diving turns would clearly increase the samples retrieving effectiveness, but these are aspects beyond our reach. Within our capacity of decision, we could have decided to do more diving immersions in any/some of the lakes, but that would have necessarily resulted into a lower number of lakes sampled. On the other hand, working with surface sediments limited the interpretation frame to a recent past (i.e. few decades). Certainly, using sediment cores representing a larger temporal sequence would increase our interpretation capability to expand the paleoreconstruction to a longer-term frame (at least centuries). The higher temporal resolution of a core versus surface sediments would offer a great perspective for assessing longer-term processes such as the effects of climate change on this poorly studied region. Indeed, this is our plan for a near future. The present study was conceived as a first approximation to the sediments biogeochemistry in the Fildes Lakes, where the study of surface sediments allowed characterizing recent sediments for their origin, preservation and transport. Future work is envisioned to investigate the molecular and isotopic profile of the long-term sedimentary record of the Fildes Peninsula lakes to reconstruct the temporal evolution and response to global warming. In a recent sampling campaign (March 2019), sediment cores of 1–1.5 m depth have been already collected from a number of lakes (including Uruguay).

5. Conclusion

Bulk geochemistry, mineralogy, isotopic and molecular biomarkers revealed different sources, oxygen conditions, and factors affecting the supply and burial of sediments in the five Fildes Lakes. Different lipid proxies and the dominance of HMW moieties reflect the importance of terrestrial carbon sources in the five surface sediments, whereas aquatic carbon sources have relatively greater weight in the Drake and Ionospheric lakes. The amount and composition of the five surface sediments suggest relative larger inputs of petrogenic carbon sources to the Drake, Ionospheric and Meltwater lakes, while dominantly biogenic to Uruguay and Kitezh. The inorganic and organic geochemistry of the sediments reveals additional information about the location and characteristics of the lacustrine watersheds. Water mixing and oxygenation is relatively poorer in the deepest Uruguay and Kitezh, where influence from the nearby coast seems to be relevant. In contrast, the well-mixed and oxygenated watersheds of Drake, Ionospheric, and Meltwater appear to be more influenced by the retreating Collins Glacier that releases ancient carbon and basaltic materials long time preserved upon freezing. Our results suggest that the geochemical signature of the surface sediments in the five lakes is largely determined by either the distance to the retreating Collin Glacier or the proximity to the coast, as well as the lake depth. The combined use of bulk, molecular, and compound-specific isotopic biomarkers allowed deciphering relevant information for reconstructing the sediments biogeochemistry the five Fildes Lakes (origin, preservation, and geochemistry), with relevance to understand future alterations and geochemical processes in this highly vulnerable system upon the current climate warming.

Appendix A. Supplementary data

Supplementary data to this article can be found online at https://doi.org/10.1016/j.scitotenv.2019.03.459.

References

Abrajano, T.A., Murphy, D.E., Fang, J., Comet, P., Brooks, J.M., 1994. $^{13}C/^{12}C$ ratios in individual fatty acids of marine mytilids with and without bacterial symbionts. Org. Geochem. 21, 611–617.

Alfonso, J.A., Vasquez, Y., Hernandez, A.C., Mora, A., Handt, H., Sira, E., 2015. Geochemistry of recent lacustrine sediments from Fildes Peninsula, King George Island, maritime Antarctica. Antarct. Sci. 27, 462–471.

Allen, M.A., Neilan, B.A., Burns, B.P., Jahnke, L.L., Summons, R.E., 2010. Lipid biomarkers in Hamelin Pool microbial mats and stromatolites. Org. Geochem. 41, 1207–1218.

Antarctic Treaty Secretariat, 2009. Fildes Peninsula, King George Island. Management Plan for Antarctic Specially Protected Area No. 125: Measure 6, Annex. https://www.ats.aq/documents/recatt/Att424_e.pdf

Arbi, I., Liu, S., Zhang, J., Wu, J., Huang, X., 2018. Detection of terrigenous and marine organic matter flow into a eutrophic semi-enclosed bay by $\delta^{13}C$ and $\delta^{15}N$ of intertidal macrobenthos and basal food sources. Sci. Total Environ. 613, 847–860. https://doi.org/10.1016/j.scitotenv.2017.09.143.

Arts, M.T., Brett, M.T., Kainz, M.J., 2009. Lipids in Aquatic Ecosystems. Springer, Dordrecht, p. 380.

Barsh, D., Mausbacher, R., 1986. New data on the relief development of the South Shetland Islands, Antarctica. Interdiscip. Sci. Rev. 11, 211–219.

Blumenberg, M., Thiel, V., Riegel, W., Kah, L.C., Reitner, J., 2012. Biomarkers of black shales formed by microbial mats, Late Mesoproterozoic (1.1 Ga) Taoudeni Basin, Mauritania. Precambrian Res. 196–197, 113–127.

Boy, J., Godoy, R., Shibistova, O., Boy, D., McCulloch, R., Andrino de la Fuente, A., Aguirre-Morales, M., Mikutta, Guggenberger, G., 2016. Successional patterns along soil development gradients formed by glacier retreat in the Maritime Antarctic, King George Island. Rev. Chil. Hist. Nat. 89, 6.

Braun, M., Saurer, H., Goßmann, H., 2004. Climate, energy fluxes and ablation rates on the ice cap of King George Island. Brazilian Antarctic Research. vol. 4, pp. 87–103.

Brocks, J.J., Summons, R.E., 2003. In: Holland, H.D., Turekian, K.K. (Eds.), Biogeochemistry. Elsevier, Amsterdam, pp. 63–115.

Cabrerizo, A., Tejedo, P., Dachs, J., Benayas, J., 2016. Anthropogenic and biogenic hydrocarbons in soils and vegetation from the South Shetland Islands (Antarctica). Sci. Total Environ. 569, 1500–1509.

Castañeda, I.S., Schouten, S., 2011. A review of molecular organic proxies for examining modern and ancient lacustrine environments. Quat. Sci. Rev. 30, 2851–2891.

Cohen, A.S., 2003. Paleolimnology: The History and Evolution of Lake Systems. Oxford University Press, New York (500 pp.).

Cranwell, P.A., 1973. Chain-length distribution of n-alkanes from lake sediments in relation to post-glacial environmental change. Freshw. Biol. 3, 259–265.

Cranwell, P.A., Eblinton, G., Robinson, N., 1987. Lipids of aquatic organisms as potential contributors to lacustrine sediments. Org. Geochem. 11, 513–527.

Di Rienzo, J.A., Casanoves, F., Balzarini, M.G., Gonzalez, L., Tablada, M., Robledo, C.W., 2018. Centro de Transferencia InfoStat, FCA, Universidad Nacional de Córdoba, Argentina. http://www.infostat.com.ar (URL, InfoStat version).

Drenzek, N.J., Montlucon, D.B., Yunker, M.B., Macdonald, R.W., Eglinton, T.I., 2007. Constraints on the origin of sedimentary organic carbon in the Beaufort Sea from coupled molecular ^{13}C and ^{14}C measurements. Mar. Chem. 103, 146–162.

Eglinton, G., Hamilton, R.J., 1967. Leaf epicuticular waxes. Science 156, 1322–1335.

Embleton-Hamann, C., 2004. Proglacial landforms. In: Goudie, A.S. (Ed.), Encyclopedia of Geomorphology. vol. 2. Routledge, London, pp. 810–813.

Fahl, K., Stein, R., 1997. Modern organic carbon deposition in the Laptev sea and the adjacent continental slope: surface water productivity vs. terrigenous input. Org. Geochem. 26, 379–390.

Ficken, K.J., Li, B., Swain, D.L., Eglington, G., 2000. An n-alkane proxy for the sedimentary input of submerged/floating freshwater aquatic macrophytes. Org. Geochem. 31, 745–749.

Freeman, K.H., Wakeham, S.G., Hayes, J.M., 1994. Predictive isotopic biogeochemistry: hydrocarbons from anoxic marine basins. Org. Geochem. 21, 629–644.

French, H.M., 2007. The Periglacial Environment. John Wiley V.C.H, Chichester (478 pp.).

Fry, B., Sherr, E.B., 1984. Delta-C-13 measurements as indicators of carbon flow in marine and fresh-water ecosystems. Contrib. Mar. Sci. 27, 13–47.

Galy, V., Peucker-Ehrenbrink, B., Eglinton, T., 2015. Global carbon export from the terrestrial biosphere controlled by erosion. Nature 521, 204–207.

Hall, B.L., Koffman, T., Denton, G.H., 2010. Reduced ice extent on the western Antarctic Peninsula at 700–970 cal yr BP. Geology 38, 635–638.

Harrison, R.M., 2007. In: Harrison, R.M. (Ed.), Principles of Environmental Chemistry. The Royal Society of Chemistry, Cambridge (UK) (363 pp.).

Hedges, J.I., Prahl, F.G., 1993. Early diagenesis: consequences for applications of molecular biomarkers. In: Engel, M.H., Mecko, S.A. (Eds.), Organic Geochemistry, Principles and Applications. Plenum Press, New York, pp. 237–253.

Hollander, D.J., McKenzie, J.A., 1991. CO_2 control on carbon-isotope fractionation during aqueous photosynthesis: a paleo-pCO_2 barometer. Geology 19, 929–932.

Hood, E., Fellman, J.B., Spencer, R.G.M., Hernes, P.J., Edwards, R.T., D'Amore, D., Scott, D., 2009. Glaciers as a source of ancient and labile organic matter to the marine environment. Nature 462, 1044–1047. https://doi.org/10.1038/nature08580.

Huang, Y., Lockheart, M.J., Logan, G.A., Eglinton, G., 1996. Isotope and molecular evidence for the diverse origins of carboxylic acids in leaf fossils and sediments from the Miocene Lake Clarkia deposit ID, USA. Org. Geochem. 24, 289–299.

Ishiwatari, R., Yamada, K., Matsumoto, K., Houtatsu, M., Naraoka, H., 1999. Organic molecular and carbon isotopic records of the Japan Sea over the past 30 kyr. Paleoceanography 14, 260–270.

Killops, S., Killops, V., 2005. Introduction to Organic Geochemistry. Blackwell Publishing, Oxford.

Lamb, A.L., Wilson, G.P., Leng, M.J., 2006. A review of coastal palaeoclimate and relative sea-level reconstructions using $\delta^{13}C$ and C/N ratios in organic material. Earth-Sci. Rev. 75, 29–57.

Lee, K., Yoon, S.K., Yoon, H.I., 2009. Holocene paleoclimate changes determined using diatom assemblages from lake Long, King George Island, Antarctica. J. Paleolimnol. 42, 1–10.

Li, S.P., Ochyra, R., Wu, P.C., Seppelt, R.D., Cai, M.H., Wang, H.-Y., Li, C.S., 2009. Drepanocladus longifolius (Amblystegiaceae), an addition to the moss flora of King George Island, South Shetland Islands, with a review of Antarctic benthic mosses. Polar Biol. 32, 1415–1425.

Machado, A., Lima, E.F., Chemale, J.F., Morata, D., Oteiza, O., Almeida, D.P.M., Figuereido, A.M.G., Alexandre, F.M., Urrutia, J.L., 2005. Geochemistry constraints of Mesozoic-Cenozoic calc-alkaline magmatism in the South Shetland arc, Antarctica. J. S. Am. Earth Sci. 18, 407–425.

Malandrino, M., Abollino, O., Buoso, S., Casalino, C.E., Gasparon, M., Giacomino, A., La Gioia, C., Mentasti, E., 2009. Geochemical characterization of Antarctic soils and lacustrine sediments from Terra Nova bay. Microchem. J. 92, 21–31.

Matsumoto, G.I., Akiyama, M., Watanuki, K., Torii, T., 1990. Unusual distributions of long-chain n-alkanes and n-alkenes in Antarctic soil. Org. Geochem. 15, 403–412.

Matsumoto, G.I., Honda, E., Sonoda, K., Yamamoto, S., Takemura, T., 2010. Geochemical features and sources of hydrocarbons and fatty acids in soils from the McMurdo dry valleys in the Antarctic. J. Polym. Sci. 4, 187–196.

Mead, R., Xu, Y.P., Chong, J., Jaffe, R., 2005. Sediment and soil organic matter source assessment as revealed by the molecular distribution and carbon isotopic composition of n-alkanes. Org. Geochem. 36, 363–370.

Mendoça, T., Melo, V.F., Schaefer, C.E.G.R., Simas, F.N.B., Michel, R.F.M., 2013. Clay mineralogy of gelic soils from the Fildes Peninsula, maritime Antarctica. Soil Sci. Soc. Am. J. 77, 1842–1851.

Meyers, P.A., 1994. Preservation of elemental and isotopic source identification of sedimentary organic matter. Chem. Geol. 144, 289–302.

Meyers, P.A., 1997. Organic geochemical proxies of paleoceanographic, paleolimnologic, and paleoclimatic processes. Org. Geochem. 27, 213–250.

Meyers, P.A., 2003. Applications of organic geochemistry to paleolimnological reconstructions: a summary of examples from the Laurentian Great Lakes. Org. Geochem. 34, 261–289.

Michel, R.F.M., Schaefer, C., Poelking, E.L., Simas, F.N.B., Fernandes, E.I., Bockheim, J.G., 2012. Active layer temperature in two Cryosols from King George Island, Maritime Antarctica. Geomorphology 155, 12–19. https://doi.org/10.1016/j.geomorph.2011.12.013.

Michel, R.F.M., Schaefer, C., Lopez-martinez, J., Simas, F.N.B., Haus, N.W., Serrano, E., Bockheim, J.G., 2014. Soils and landforms from Fildes Peninsula and Ardley Island, maritime Antarctica. Geomorphology 225, 76–86.

Monien, P., Schnetger, B., Brumsack, H.J., Hass, H.C., Khun, G., 2011. A geochemical record of late Holocene palaeoenvironmental changes at King George Island (maritime Antarctica). Antarct. Sci. 23, 255–267.

Nna-Mvondo, D., Martin-Redondo, M.P., Martinez-Frías, J., 2008. New application of microwave digestion-inductively coupled plasma-mass spectrometry for multi-element analysis in komatiites. Anal. Chim. Acta 628, 133–142.

Nott, C.J., Xie, S., Avsejs, L.A., Maddy, D., Chambers, F.M., Evershed, R.P., 2000. n-Alkane distributions in ombrotrophic mires as indicators of vegetation change related to climatic variation. Org. Geochem. 31, 231–235.

Ouyang, X., Guo, F., Bu, H., 2015. Lipid biomarkers and pertinent indices from aquatic environment record paleoclimate and paleoenvironment changes. Quat. Sci. Rev. 123, 180–192.

Pancost, R.D., Boot, C.S., 2004. The palaeoclimatic utility of terrestrial biomarkers in marine sediments. Mar. Chem. 92, 239–261.

Parro, V., Diego-Castilla, G., Moreno-Paz, M., Blanco, Y., Cruz-Gil, P., Rodríguez-Mandredi, J.A., Férnandez-Remolar, D., Gómez, F., Gómez, M.J., Rivas, L.A., Demergasso, C., Echeverría, A., Urtuvia, V.N., Ruiz-Bermejo, M., García-Villadangos, M., Postigo, M., Sánchez-Román, M., Chong-Díaz, G., Gómez-Elvira, J., 2011. A microbial oasis in the hypersaline Atacama subsurface discovered by a life detector chip: implications for the search of life on Mars. Astrobiology 11, 969–996.

Peter, H.U., Buesser, C., Mustafa, O., Pfeifer, S., 2008. Risk assessment for the Fildes peninsula and Ardley Island, and development of management plans for their designation as Specially Protected or Specially Managed Areas. Research Report 203 12 124 UBA-FB 001155e (508 pp.).

Peters, K.E., Walters, C.C., Moldowan, J.M., 2005. The Biomarker Guide - Part II - Biomarkers and Isotopes in Petroleum Exploration and Earth History. Cambridge University Press, New York.

Prahl, F.G., Bennett, J.T., Carpenter, R., 1980. The early diagenesis of aliphatic hydrocarbons and organic matter in sedimentary particles from Dabob Bay, Washington. Geochim. Cosmochim. Acta 44, 1967–1976.

Prus, W., Fabianska, M.J., Labno, R., 2015. Geochemical markers of soil anthropogenic contaminants in olar scientific stations nearby (Antarctica, King George Island). Sci. Total Environ. 518, 266–279.

Quayle, W.C., Peck, L.S., Peat, H., Ellis-Evans, J.C., Harrigan, P.R., 2002. Extreme responses to climate change in Antarctic lakes. Science 295, 645.

Révész, K., Qi, H., and Coplen, T.B., 2012. Determination of the δ15N and δ13C of total nitrogen and carbon in solids. RSIL lab code 1832, chap. 5 of Stable isotope-ratio methods, sec. C of Révész, Kinga, and Coplen, T.B. eds. Methods of the Reston Stable Isotope Laboratory (slightly revised from version 1.1 released in 2007): U.S. Geological Survey Techniques and Methods, book 10, 31 p., available only at https://pubs.usgs.gov/tm/2006/tm10c5/. (Supersedes versions 1.0 and 1.1 released in 2006 and 2007, respectively.)

Rieley, G., Collier, R.J., Jones, D.M., Eglinton, G., 1991. Biogeochemistry of Ellesmere Lake, U.K. I. Source correlation of leaf wax inputs to the sedimentary lipid record. Org. Geochem. 17, 901–912.

Robinson, D., 2001. δ15N as an integrator of the nitrogen cycle. Trends Ecol. Evol. 16, 153–162.

Robinson, N., Eglinton, G., Brassell, S.C., Cranwell, P.A., 1984. Dinoflagellate origin for sedimentary 4-alpha-methylsteroids and 5-alpha(H)-stanols. Nature 308, 439–442.

Sánchez-García, L., Aeppli, C., Parro, V., Fernandez-Remolar, D., García-Villadangos, M., Chong-Díaz, G., Blanco, Y., Carrizo, D., 2018. Molecular biomarkers in the subsurface of the Salar Grande (Atacama, Chile) evaporitic deposits. Biogeochemistry 140, 31–52.

Serrano-Cañadas, E., 2003. Paisaje Natural y pisos geoecológicos en las áreas libres de hielo de la Antártida marítima: Islas Shetland del Sur. Boletín de la A.G.E. N.° 35, 5–32.

Simoneit, B.R.T., Sheng, G., Chen, X., Fu, J., Zhang, J., Xu, Y., 1991. Molecular marker study of extractable organic matter in aerosols from urban areas of China. Atmos. Environ. 10, 2111–2129.

Skidmore, M.L., Foght, J.M., Sharp, M.J., 2000. Microbial life beneath a high arctic glacier. Appl. Environ. Microbiol. 66, 3214–3220.

Smellie, J.L., Pankhurst, R., Thomson, M.R.A., Davies, R.E.:S., 1984. The geology of the South Shetland Islands, VI. Stratigraphy, geochemistry and evolution. British Antarctic Survey Scientific Report, No. 87 (85 pp.).

Thiel, V., Merz-preiβ, M., Reitner, J., Michaelis, W., 1997. Biomarker studies on microbial carbonates: extractable lipids of a calcifying cyanobacterial mat (Everglades, USA). Facies 36, 163–172.

Thomas, E.R., Tetzner, D.R., 2018. The climate of the Antarctic Peninsula during the twentieth century: evidence from ice cores. In: IntechOpen (Ed.), Antarctica - A Key to Global Change https://doi.org/10.5772/intechopen.81507 (18 pp.).

Torres-Mellado, G.A., Jana, R., Casanova-Katny, M.A., 2011. Antarctic hairgrass expansion in the South Shetland archipelago and Antarctic Peninsula revisited. Polar Biol. 34, 1679–1688.

van Dongen, B.E., Semiletov, I., Weijers, J.W.H., Gustafsson, Ö., 2008. Contrasting lipid biomarker composition of terrestrial organic matter exported from across the Eurasian Arctic by the five Great Russian Arctic Rivers. Global Biogeochem. Cy. 22, GB1011. https://doi.org/10.1029/2007GB002974.

Vera, L., Fernandez-Turiel, T., Quesada, A., 2013. A distribution and reproductive capacity of Dechampsia antarctica and Colobanthus quitensis on Byers Peninsula, Livingston Island, South Shetland Islands, Maritime Antarctica. Antarct. Sci. 25, 292–302.

Vieira, R., Marotta, H., Kellem da Rosa, K., Jaña, R., Lorenz-Simoes, C., de Souza-Junior, E., Ferreira, F., Ronquette-Santos, L., dos Santos, J.V., Perroni, M.A., Goncalves, M., Farias-Santos, J.P., Rodrigues, R.I., Medieros Galvao, J.C., de Sá Felizardo, J.P., 2015. Análisis Sedimentológico y geomorfológico de áreas lacustres en la Península Fildes, Isla Rey Jorge, Antártica Marítima (in Spanish). Investig. Geogr. Chile 49, 03–33.

Vogts, A., Moossen, H., Rommerskirchen, F., Rullkotter, J., 2009. Distribution patterns and stable carbon isotopic composition of alkanes and alkan-1-ols from plant waxes of African rain forest and savanna C3 species. Org. Geochem. 40, 1037–1054.

Xianshen, Z., Xiaohan, L., 1990. Geology of volcanic rocks on Fildes Peninsula, King George Island. West Antarctica. Chin. J. Polar Res. 1, 8–19.

Xu, Y., Simpson, A.J., Eyles, N., Simpson, M.J., 2010. Sources and molecular composition of cryoconite organic matter from the Athabasca Glacier, Canadian Rocky Mountains. Org. Geochem. 41, 177–186.

Yunker, M.B., Macdonald, R.W., Veltkamp, D.J., Cretney, W.J., 1995. Terrestrial and marine biomarkers in a seasonally ice-covered Arctic estuary — integration of multivariate and biomarker approaches. Mar. Chem. 49, 1–50.